Int. J. Electrochem. Sci., 5 **(2010)** 278 - 294

International Journal of
ELECTROCHEMICAL
SCIENCE
www.electrochemsci.org

Comparative Studies of the Electrochemical Behavior of Silver Electrode in Chloride, Bromide and Iodide Aqueous Solutions

Hamdy H. Hassan. Magdy A. M. Ibrahim. Sayed S. Abd El Rehim. Mohammed A. Amin

Faculty of Science, Chemistry Department, Ain Shams University, 11566 Abbassia, Cairo, Egypt
*E-mail: maaismail@yahoo.com

Received: 1 February 2010 / *Accepted:* 25 February 2010 / *Published:* 1 February 2010

Comparative studies of the electrochemical behaviour of Ag in aqueous NaCl, NaBr and NaI solutions of various concentrations ranging from 0.1 M to 1.0 M have been made by means of cyclic voltammetry and chronoamperometry techniques, complemented with SEM observation. The cyclic voltammograms of Ag in the three halide solutions are nearly similar and characterized by the occurrence of a broad anodic peak (AI) corresponding to the electroformation of AgX film (X^- = Cl^-, Br^-, I^-) and a sharp cathodic peak (CI) corresponding to the electroreduction of AgX to Ag. The peak current density of peak AI decreases in the order $I^- > Br^- > Cl^-$. The electroformation of AgX is found to be limited by the diffusion of X^- ions from the bulk of the solution to the electrode surface. The apparent activation energies required for the electroformation of AgX films and its electroreduction were calculated from Arrhenius plots. It was found that, the activation energies decrease in the order: $Cl^- > Br^- > I^-$. Potentiostatic current/time transients show that the instantaneous and steady-state current densities increase by increasing either the anodic step potential ($E_{s,a}$), solution concentration, or temperature. SEM examination for AgX films indicates that, the AgI film is highly porous and associated with large microcracks as compared to AgBr and AgCl films.

Keywords: Anodic Dissolution. Silver Electrode. Halides Solutions. Cyclic Voltammetry. Chronoamperometry

1. INTRODUCTION

A considerable amount of research has involved silver electrodes in different media. The interest in the electroformation and electroreduction of insoluble silver salts in different electrolytes containing halides, hydroxides, carbonates, chromates, perchlorate, etc.[1-6] and the particular aspects of their electrochemistry is based mainly on the relevance that these films have in galvanic cells, sea-water batteries, second class reference electrodes and corrosion and passivation [7]. Moreover, the

corrosion and passivation of Ag electrode in biological and physiological solutions has been made [8,9].

The electroformation of AgCl during electrooxidation of Ag in neutral NaCl solution was investigated [10] by using potentiostatic and potentiodynamic techniques. The authors demonstrated that, the kinetics of the electroformation of AgCl is interpreted through a complex model that implies the formation of adsorbed AgCl species at the submonolayer level. The electrodissolution of Ag through the AgCl submonolayer takes place via the formation of a complexing ion that diffuses out of the electrode. Birss et al. [11,12] studied the potentiodynamic formation of AgBr and AgI on a silver rotating disc electrode in aqueous bromide and iodide solutions respectively. They found that, the halide film growth is limited by physical parameters such as ionic diffusion and migration in the solution. They further concluded that, the halide film formation occurs initially by the nucleation of islands of film to a critical thickness, and then this islands spread laterally until only small pores remain between them.

The galvanostatic formation of AgX films was initially studied by Kurtz [13], who found AgCl and AgBr films to be highly porous when formed at high current densities. On the basis of galvanostatic and microscopic examinations, Briggs et al. [14], Jaenicke et al., [15,16] and Awad [17] reported that AgCl films, as well as the reduced Ag, are porous. Fleischmann and Thirsk [18] also found that AgCl deposits which were formed galvanostatically on Ag were generally non-passivating. Vermilyca [19] has considered films of AgX on silver anode as non continuous films. Some of the metal substrate is exposed and ions diffuse to and from the metal through openings in the overlaying salt.

The little work published on the electrochemical behaviour of Ag in aqueous NaCl, NaBr, and NaI solutions promotes us to throw more light onto the cyclic voltammetric behaviour of Ag electrode in these solutions and to make a comparative study between them. It was also the purpose of the present work to study the growth kinetics of AgX films by means of potentiostatic current/time measurements.

2. EXPERIMENTAL PART

The working electrode employed in the present study was made of pure polycrystalline silver (99.99%, Koch light laboratories, colnbrook Bucks England) axially embedded in an Araldite holder to offer an active flat disc shaped surface of area 0.1256 cm^2. Prior to each experiment, the working electrode was polished successively with fine grade emery papers, then the polished metal surface was rinsed with acetone, distilled-water, and finally dipped in the electrolytic cell. A platinum wire was used as the counter electrode. A saturated **c**alomel electrode (SCE) was used as a reference electrode to which all potentials are referred. In order to avoid X^- (X^- = Cl^-, Br^-, and I^-) diffusion in the cell, the reference electrode was connected to the working electrode through a bridge filled with the solution under test, the capillary tip of the bridge being very close to the surface of the working electrode to minimize the i.R drop. All solutions were prepared from analytical grade chemical reagents using doubly distilled water and were used without further purification. For each run, a freshly prepared

solution as well as a cleaned set of electrodes were used. Each run was carried out in aerated stagnant solution at the required temperature ± 1 ^{o}C.

Potentiodynamic cyclic polarization experiments were employed using an EG & G Potentiostat/Galvanostat Model 273 connected to a personal computer using the EG &G M352 corrosion software. The experiments were carried out by changing the electrode potential automatically from the starting potential, $E_{s,c}$, towards more positive direction at required scan rate till the final potential, $E_{s,a}$,then the scan is reversed towards the starting potential, $E_{s,c}$, again. The microstructure of the surface of the Ag electrode pretreated as above and potentiodynamically polarized from -2.0V up to 0.5V at a scan rate of 100 mV s^{-1} and 25^{o}C in 0.5M NaCl, NaBr and NaI separate solutions were tested using scanning electron microscope model JOEL - JEM - 1200 EX II Electron microscope.

The potentiostatic current/time transients were recorded for Ag electrode in NaX solutions at a constant anodic potential ($E_{s,a}$) under the influence of various experimental variables. The measurements were carried out after a two step procedure namely: the working electrode was first held at the starting potential for 60 s to attain a reproducible electroreduced electrode surface. Then the electrode was suddenly polarized in the positive direction to an anodic step potential $E_{s,a}$ at which the current transient was recorded.

3. RESULTS AND DISCUSSION

Figure 1 shows the first cyclic voltammograms for polycrystalline Ag electrode in 0.3 M NaCl, NaBr and NaI aqueous solutions recorded between $E_{s,c}$ = - 2.0 and $E_{s,a}$ = 2.0 V (SCE) at 25°C and at a scan rate of 100 mV s^{-1}. The data show that in all halide solutions, the curves have nearly the same general features. At the starting potential, $E_{s,c}$, hydrogen evolution commences kinetically important. On positive going scan, the cathodic current density decreases gradually up to zero current potential $E_{i=0}$ where it changes its sign. The anodic current density increases initially linearly with the applied potential, and then forms a broad anodic current peak AI corresponding to the formation of AgX (X= Cl^{-}, Br^{-} or I^{-}) solid phase on the anode surface. Beyond the peak AI, the passive current density "$i_{pass.}$" decreases slightly with the applied potential up to 2.0 V without any sign for oxygen evolution.

The values of "$i_{pass.}$" are relatively high ($i_{pass.}$ = 10 mA cm^{-2}) indicating porous nature of the formed AgX layer. Birss et al [11,12] suggested that, the halide film (bromide and iodide) occurs initially by the nucleation of islands of AgX to a critical thickness, and then these islands spread laterally until only small pores remain between them. Vermilyca [19] has considered films of AgX on silver anode as non continuous films. Therefore, some of the metal surface is exposed and X^{-} ions diffuse to the metal through pores in the overlaying salt.

For NaCl and NaBr solutions, on reversing the potential scan, the passivation current density decreases gradually till the potential $E_{i\,=\,0}$. During potential region, part the formation of AgX is continued. However, for NaI solution, a small activation anodic current peak AII is observed during the reverse potential scan. This peak suggests the occurrence of a reactivation process. Although, the

peak AII is not observed in the previous work of Birss et al. [12], its appearance here confirms their suggestion that the anodic surface of Ag in NaI solution is not fully covered by AgI film under the prevailing conditions. A cathodic current peak CI is observed in the three halide solutions. The appearance of this cathodic peak is related to the electroreduction of the AgX film to Ag. The charge consumed in anodic formation of AgX (anodic peak AI and its plateau and the anodic part of the reverse scan) is nearly equal to the charge involved in the cathodic reduction of AgX. This indicates that, all of the anodically formed AgX is cathodically reduced in the potential range of the peak CI.

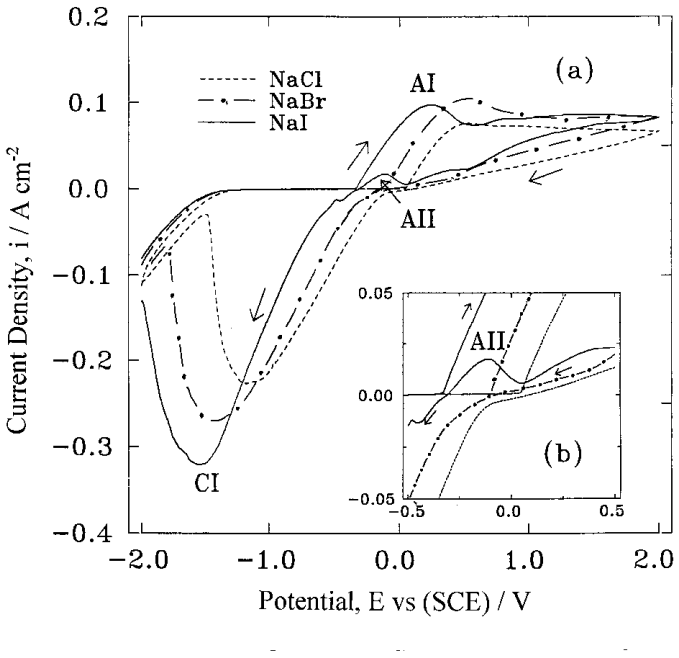

Figure 1. (a) Typical first cyclic voltammograms for polycrystalline Ag electrode recorded in 0.30 M NaCl, NaBr and NaI solutions between $E_{s,c}$ = - 2.0 and $E_{s,a}$ = 2.0 V (SCE) at 25°C and scan rate of 100 mV s^{-1}. (b) a zoom in at the region of activated anodic peak AII.

It is probable that, the initial stage of anodic process of Ag in NaX solutions involves the participation of chemically adsorbed halide ions in ionization of Ag atoms and formation of soluble complexes which diffuse out from the electrode surface as follows [11,12]:

$$\begin{aligned} Ag + X^-_{(ads.)} &= AgX_{(ads.)} + e \\ AgX_{(ads.)} + (n-1)X^- &= AgX^{-(n-1)}_{n\ (ads.)} \\ AgX^{-(n-1)}_{n\ (ads.)} &= AgX^{-(n-1)}_{n\ (aq.)} \end{aligned} \qquad (2)$$

where $0 < n \leq 3$

The second level of anodic process involves the participation of the complex ions in nucleation of AgX film according to the reaction :

$$AgX^{-(n-1)}_{n\ (aq.)} = AgX_{(aq.)} + (n-1)X^- \qquad (4)$$

This reaction is followed by precipitation of AgX on the anode surface:

$$AgX_{(aq.)} = AgX_{(s)} \quad (5)$$

On the other hand, the electroreduction of the anodically formed $AgX_{(s)}$ on the electrode surface occurs by an opposite path: dissolution of $AgX_{(s)}$ most probably along their boundaries followed by their diffusion and charge transfer reaction on the bare Ag surface as described by the following sequences of reactions:

$$(n-1)X^- + AgX_{(s)} = AgX_{n\ (ads.)}^{-(n-1)}$$
$$AgX_{n\ (ads.)}^{-(n-1)} = AgX_{n\ (aq.)}^{-(n-1)} \quad (7)$$
$$AgX_{n\ (aq.)}^{-(n-1)} + e = Ag + (n-1)X_{(aq.)}^-$$

The presence of excess of X^- ions in the solution enhances the solubilities of AgX by the formation of the soluble complexes $AgX_{n\ (aq.)}^{-(n-1)}$. Such complexing process leads to a decrease in the free Ag^+ ion concentration at the electrode surface and consequently a delay in the precipitation of AgX and an increase in the values of both i_{AI} (peak current density of peak AI) and $i_{pass.}$.

Table 1. Activation parameters for the dissolution reaction of polycrystaline Ag electrode in 0.5 M NaCl, NaBr and NaI solutions (calculated from potentiodynamic tests).

Electrolytic Solution	**E*/kJ mol^{-1}**		**ΔH*/ kJ mol^{-1}**		**ΔS*/ J K^{-1}.mol^{-1}**	
	Anodic	**Cathodic**	**Anodic**	**Cathodic**	**Anodic**	**Cathodic**
NaCl	3.8	4.4	6.1	7.7	105.4	99.3
NaBr	2.7	4.1	3.6	6.8	107.8	99.7
NaI	2.4	3.9	3.2	6.3	108.4	100.1

Inspection of the data in Fig. 1 reveals also that, at the same concentration of halide solution, the peak potentials E_{AI} of peak AI of Ag in NaI solution are more negative than those for Ag in NaBr and NaCl solutions (Table 1). This shift in peak potentials with the identity of the halide ions is related primary to the different redox potentials of the three halide solutions. This trend agrees with the standard potentials of the corresponding reactions [20]:

$$Ag + I^- = AgI + e \qquad E^o = -15\ mV \quad (9)$$
$$Ag + Br^- = AgBr + e \qquad E^o = 30\ mV \quad (10)$$
$$Ag + Cl^- = AgCl + e \qquad E^o = 222\ mV \quad (11)$$

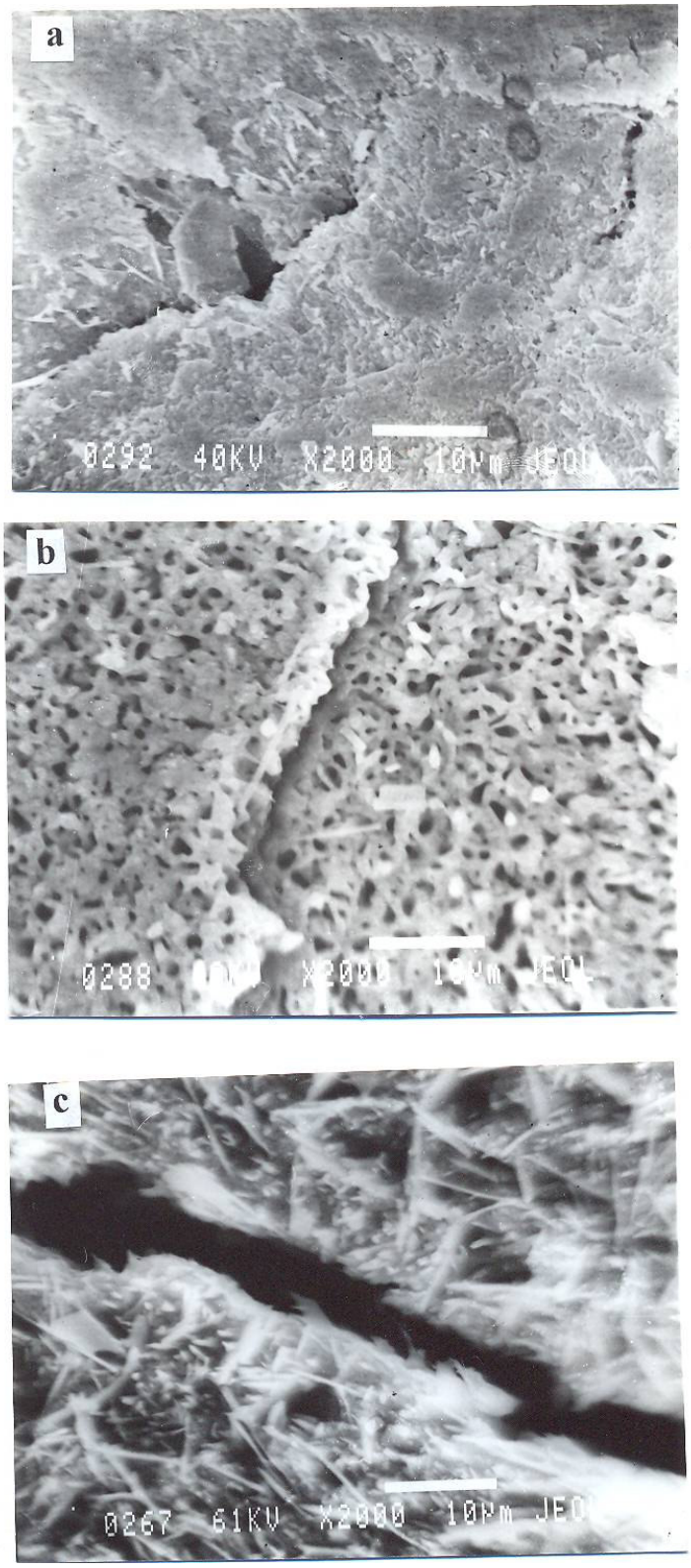

Figure 2. SEM micrographs for polycrystalline Ag electrode potentiodynamically polarized from -2.0V up to 0.5V at a scan rate of 100 mV s^{-1} and at 25^{o}C in 0.50 M NaCl (a), NaBr (b) and NaI (c).

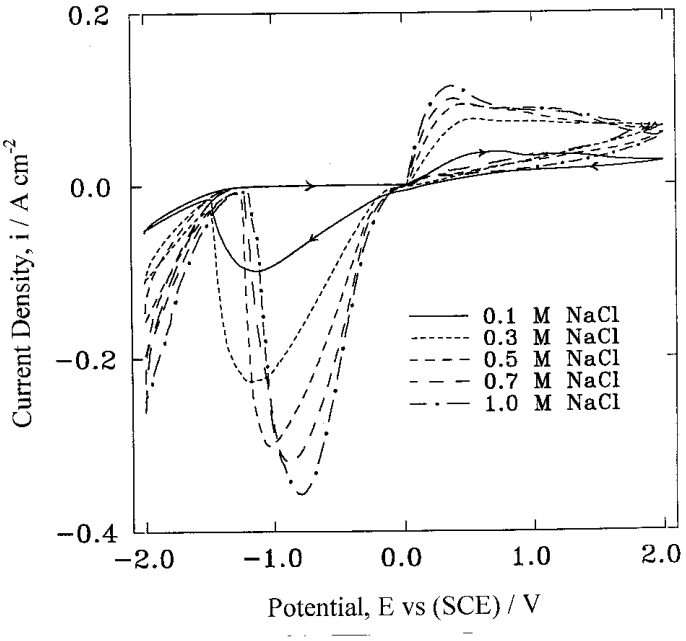

Figure 3. Typical first cyclic voltammograms for polycrystalline Ag electrode in different concentrations of NaCl solutions recorded between $E_{s,c}$ = - 2.0 and $E_{s,a}$ = 2.0 V (SCE) at 25°C and scan rate of 100 mV s^{-1}.

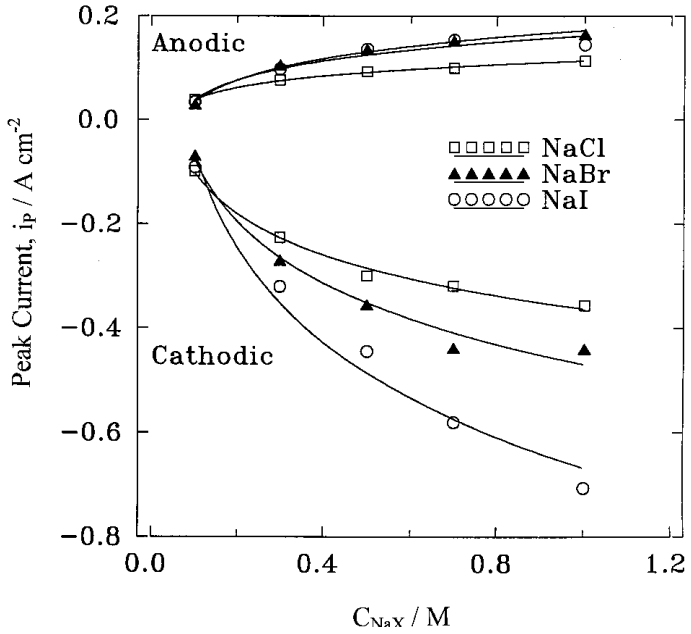

Figure 4. Dependence of peak current densities (i_P = i_{AI} for the anodic peak and i_{CI} for the cathodic peak) on the concentration of halide solution C_{NaX} for polycrystalline Ag electrode in NaX solutions at 25°C and at a scan rate of 100 mV s^{-1}.

Such trend could be explained on the basis of specific adsorption of these halides on the Ag metal surface. It is known that the halide ions are likely to become chemically adsorbed on Ag surface forming a potentially active dissolution sites. Therefore, the higher aggressiveness of I^- is partly related to higher adsorbability expected for I^- as compared to Br^- and Cl^- as deduced from their respective polarizabilities [21]. In addition, the higher aggressiveness of I^- ions is also due to the higher stability of the soluble $AgI_n^{-(n-1)}$ as compared to $AgBr_n^{-(n-1)}$ and $AgCl_n^{-(n-1)}$ [20]. Consequently, the delay in the precipitation of AgX on the anode surface (i_{AI}) is in the sequence of AgI > AgBr > AgCl.

Accordingly, it is expected that the formed AgI layer is the most porous and thinnest layer. SEM examination for AgX films formed potentiodynamically on Ag anode surface supports the suggestion that, the AgI film is highly porous and associated with large microcracks as compared to AgBr and AgCl (Fig. 2). The appearance of the activated anodic peak AII in NaI solution (Fig.1a) could be due to general weakening of the resulted AgI layer.

3.1. Effect of NaX concentration

Figure 3 shows the first cyclic voltammograms for polycrystalline Ag electrode in various concentrations (ranging from 0.1 M to1.0 M) of NaCl recorded between $E_{s,c}$= -2.0 and $E_{s,a}$= 2.0 V (SCE) at 25°C and at a scan rate of 100 mV s^{-1}. Similar results are obtained for the Ag electrode in NaBr and NaI solution (votlammograms are not shown here). The relationship between peak current densities i_p (i_p= i_{AI} for anodic peak AI and i_{CI} for cathodic peak CI) and C_{NaX} is shown in Fig. 4. Inspection of the data implies that, both i_{AI} and i_{CI} enhances with increasing the halide ion concentration [X^-]. Increasing halide concentration leads to higher surface coverage of the electrode during the anodic part of the voltammogram by the AgX film (larger amount of AgX) [12] which can explain the increase in i_{CI} with increasing the halide concentration. Moreover, an increase in solution concentration shifts the peak potential E_{AI} of peak AI to more negative potentials and that of peak CI (E_{CI}) to more positive potentials. It is found that the values of the peak potential differences ΔE_P (ΔE_P = anodic peak potential (E_{AI}) - cathodic peak potential (E_{CI})) are high, indicating the irreversible nature of the processes. However, increasing halide concentration decreases ΔE_P. This can be attributed to the lower values of solution resistance for concentrated solutions which leads to a smaller i.R drop that can explain the negative shift of the anodic peak potentials (E_{AI}) and the positive shift of the cathodic peak potentials (E_{CI}) and consequently the smaller values of ΔE_P.

3.2. Effect of anodic potential scan limit

Figure 5 shows the first cyclic voltammograms for Ag electrode recorded in 0.5 M NaCl solution at 25°C and at scan rate of 100 mV s^{-1}. The voltammograms were started from $E_{s,c}$ = -2.0 V and reversed at various anodic step potentials $E_{s,a}$ in order to inspect complementary the anodic and cathodic reactions. Similar results are obtained for Ag electrode in 0.5 M NaBr and NaI solutions (curves are not given here). The shape of the reversed potential scan depends remarkably on $E_{s,a}$. Inspection of the data depicts that, in the three halide solutions, when $E_{s,a}$ is reversed within the initial

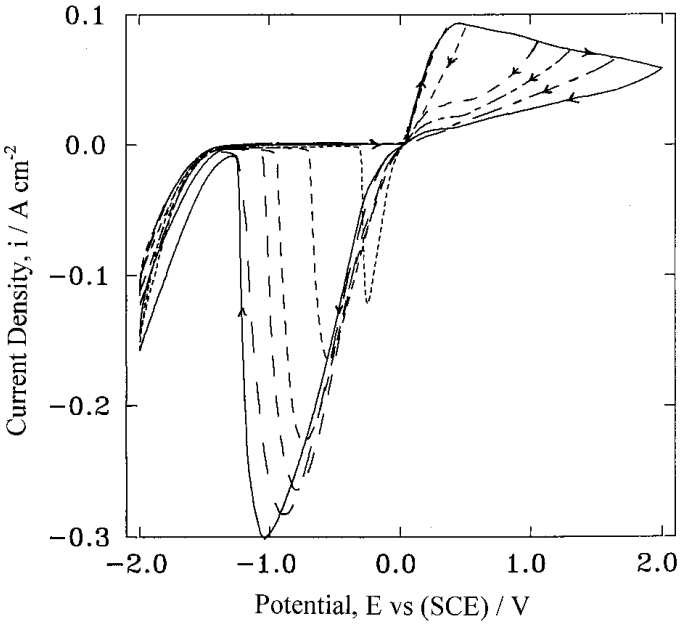

Figure 5. Typical first cyclic voltammograms for polycrystalline Ag electrode recorded in 0.50 M NaCl solution at 25°C and at a scan rate of 100 mV s^{-1} starting from $E_{s,c}$ = -2.0V and reversed at various anodic potentials.

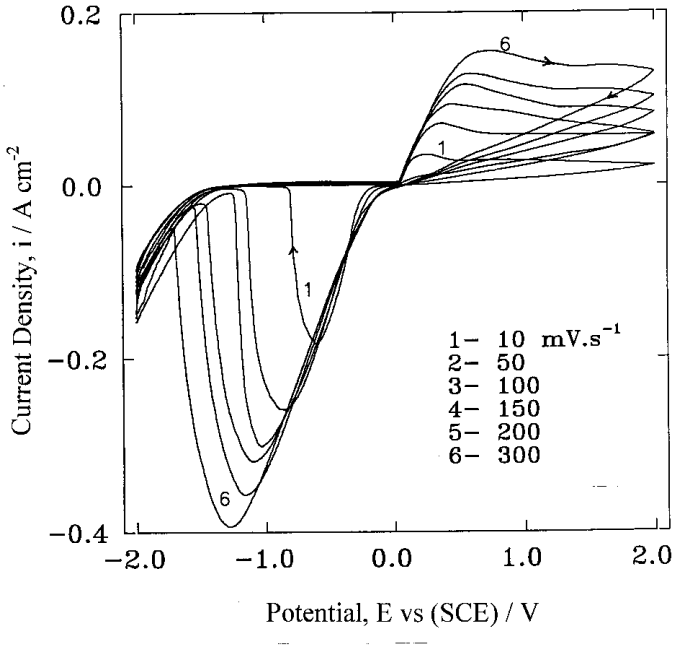

Figure 6. Typical first cyclic voltammograms for polycrystalline Ag electrode recorded in 0.50 M NaCl solution between $E_{s,c}$ = - 2.0 and $E_{s,a}$ = 2.0 V (SCE) at 25°C and at various scan rates.

potential range on the arising part of the anodic peak AI, the reverse scan retraces itself and does not display cathodic peak indicating that, the electrode surface in this potential range is free from any AgX layer. Birss et al [11,12] concluded that, the anodic process of Ag in NaBr and NaI solutions in the initial potential range is controlled only by physical processes such as migration of ions in solution and the diffusion of halide ion to the electrode surface. However, when $E_{s,a}$ is in the final range of the arising part of the peak AI, the reverse potential scan retraces part of the forward scan and finally yields a small cathodic peak CI indicating the existence of AgX film on the anode surface. It is observed that in NaCl and NaBr solutions where $E_{s,a}$ exceeds the potentials of the anodic peak AI, the reverse potential scan exhibit only the cathodic peak CI, while in NaI solutions, the reverse potential scan exhibits the activated anodic peak AII in addition to the cathodic peak CI. It is worth noting that the cathodic peak current density i_{CI} increases and its peak potential E_{CI} drifts to more negative direction as $E_{s,a}$ becomes more positive. It seems that the increase in $E_{s,a}$ enhances the stability and protectiveness of the anodically formed AgX layers as a result of increasing their thickness.

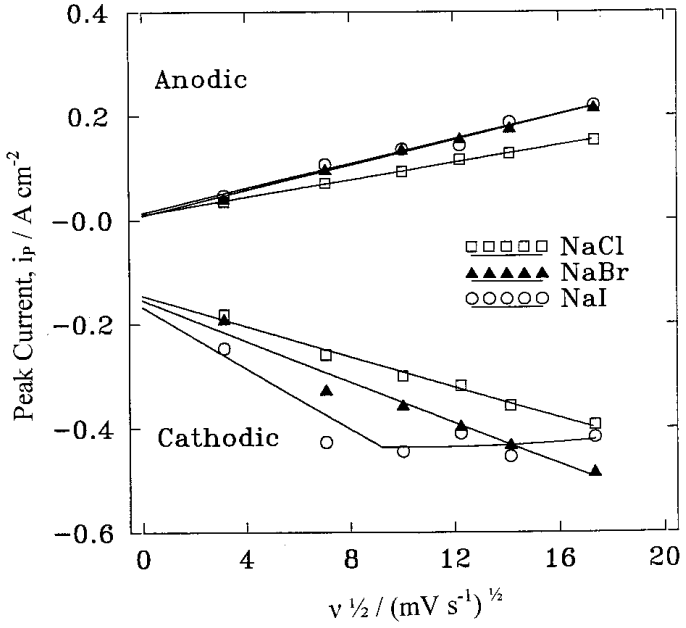

Figure 7. Dependence of peak current densities (i_P) on the square root of scan rate $\nu^{1/2}$ for the Ag electrode in 0.50 M NaX solutions at 25°C.

3.3. Effect of potential scan rate

The influence of scanning rate ν (10 - 300 mV s^{-1}) on the first cyclic voltammetric behaviour of Ag electrode was studied in 0.5 M NaCl solution (Fig.6). Similar results were obtained for NaBr and NaI solutions (data are not included here). Inspection of the data of Fig. 6 reveals that, the peak current densities ($i_p = i_{AI}$ or i_{CI}) increase with increasing the potential scan rate ν. Fig. 7 displays linear relationships between peak current densities and $\nu^{1/2}$. The anodic lines pass through the origin, while

the cathodic ones don't. These results indicate that, the electroformation of Ag surface layer are limited simply by diffusion of X^- ions from the bulk of the solution to the electrode surface and the cathodic dissolution of AgX layer is not a pure diffusion controlled process. For a pure diffusion controlled process under potentiodynamic conditions, the slope of the linear relation of i_p vs. $\nu^{1/2}$ is proportional to the concentration of the diffusing species (C) and to the square root of its diffusion coefficient (D) according to the following equation [21]:

$$i_p = a.b.z^{1/2}.C.D^{1/2}.\nu^{1/2} \quad (12)$$

where a and b are constants, z is the number of exchanged electrons. Nevertheless, the peak potential E_{AI} shifts towards the more positive direction while the peak potential E_{CI} moves towards the more negative direction indicating an increase in the peak potential difference ΔE_P with increasing ν.

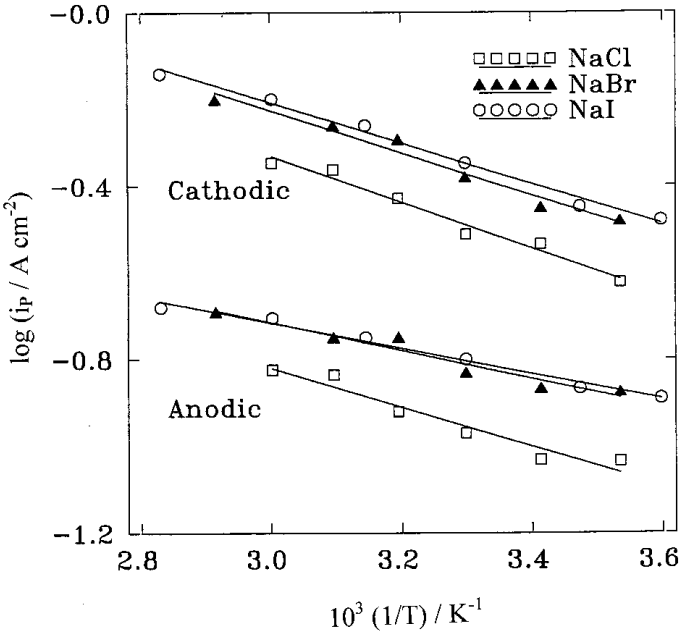

Figure 8. The relation between logarithm of the absolute values of i_P and the reciprocal of the absolute temperature for Ag electrode in 0.5M NaX at scan rate of 100 mV s^{-1} (Arrhenius plots).

3.4. Effect of temperature

The influence of changing the solution temperature (T = 5 - 80°C) on the first cyclic voltammograms for Ag electrode in 0.5 M NaCl, NaBr and NaI solutions was studied. The relationships between log $|i_P|$ vs. (1/T) for the three halide solutions are given in Fig. 8 according to the Arrhenius equation (13):

$$\log (Rate) = -E^* / 2.303RT + A \quad (13)$$

where E* is the apparent activation energy and A is a constant. It was found that, both i_{AI} and i_{CI} increase by increasing temperature. The increase in solution temperature accelerates the diffusion rate of X^- ions to the metal surface giving rise to larger amounts of AgX solid phase. Therefore, one can expect an increase in i_{CI} with temperature. The apparent activation energies E* were calculated from the slopes of the straight lines of Fig. 8 and their values are given in Table 2. These activation energies are assigned to the transport of X^- ions through AgX layer. The lower activation energy for Ag in NaI (2.4 kJ mol^{-1}) solution reflects the high porous nature of AgI film as compared to AgBr (2.7 kJ mol^{-1}) and AgCl (3.8 kJ mol^{-1}) films. The other thermodynamic functions (ΔS^* and ΔH^*) of anodic and cathodic processes of Ag electrode in 0.5 M NaX were obtained by applying the transition state equation (14) respectively:

$$\text{Rate} = RT / Nh \exp(\Delta S^*/R) \exp(\Delta H^*/RT) \qquad (14)$$

where ΔS^* is the entropy of activation, ΔH^* is the enthalpy of activation, h is the Plank's constant and N is the Avogadro's number. According to equation (14) a plot of log (Rate/T) vs 1/T should give straight line with a slope of ($-\Delta H^*/2.303R$) and an intercept of ($\log(R/Nh) - \Delta S^*/2.303R$). The calculated parameters are given in Table 2. The large positive values of the entropy of activation ΔS^* implies that the activated complex in the rate determining step represents a dissociation rather than an association step. This means that, an increase in disordering takes place on going from reactants to the activated complex [22, 23]. Moreover, it is found that an increase in temperature shifts the peak potential E_{AI} shifts to more negative values while E_{CI} shifts to more positive direction (i.e., ΔE_P decreases) with increasing temperature. This potential shift is caused by decreasing the solution resistance and consequently the i.R drop decreases with temperature.

Table 2. Values of the slopes of the lines for Ag electrode in 0.30 M NaX solution at 25°C under the influence of increasing $E_{s,a}$.

	Slope (P)		
$E_{s,a}$ / V	**Cl^-**	**Br^-**	**I^-**
0.50	1.32	1.65	2.01
0.60	1.97	2.36	2.98
0.70	2.02	2.75	3.24
0.80	3.55	4.87	5.95
0.90	4.79	6.24	7.89
1.00	7.16	8.14	9.70

3.5. Effect of repetitive cycling

Figure 9 shows typical cyclic voltammograms characteristics for Ag electrode recorded in 0.5 M NaCl solution at 25°C and at a scan rate of 100 mV s^{-1} under the influence of successive cycling between $E_{s,c}$= -2.0V and $E_{s,a}$ = 2.0V (SCE). Similar results were obtained in both NaBr and NaI

solutions (results aren't given here). The data reveal that, upon successive cycling, not only significant changes are observed in the relative amplitude (i.e., the peak heights), but also in the position of the various peaks (i.e., the peak potentials). After about six cycles a stable voltammograms emerge. A feature worthy of attention is that, the amount of charges consumed through the anodic and cathodic peaks increase with repetitive cycling. This feature is due to the fact that, on repeating cycling, the AgX products formed during the anodic potential span are reduced to Ag during the consequent cathodic potential span. Therefore, it is possible that the surface area of the Ag electrode increases progressively with repetitive cycling as a result of increasing surface roughness. Inspection of Fig. 11 also shows that, the peak potential difference ΔE_P increases with successive cycling, such increase in ΔE_P may be due to the effect of changes in the surface roughness [2,3], where increasing surface roughness leads to higher current which results in higher i.R drop.

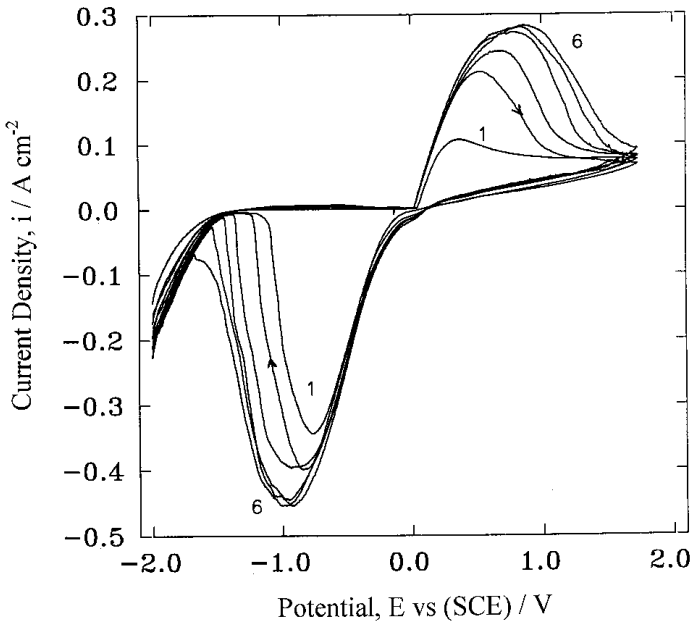

Figure 9. Effect of repetitive cycling (6 cycles) on the voltammetric response for polycrystalline Ag electrode in 0.50 M NaCl solution at 25°C and at scan rate of 100 mV s^{-1}.

3.6. Current/time transient measurements

In order to gain more information about the growth kinetics of AgX films, potentiostatic current/time transients were performed for Ag electrode in NaX solutions under various experimental conditions. A series of current/time transients at constant anodic step potentials ($E_{s,a}$) in the potential range $0.50 \leq (E_{s,a}) \leq 1.0$ V (SCE) for a Ag electrode in 0.30 M NaX solutions at 25°C were recorded after a two-step procedure. The Ag electrode was first held at $E_{s,c}$ = -2.0 V for 60 s to attain a reproducible electroreduced Ag surface, and then the electrode was immediately stepped to an anodic potential ($E_{s,a}$) at which the current transient was recorded as a function of time. Fig. 10 shows the

current/time transients obtained for Ag electrode in 0.30 M NaCl solution at 25°C and at different $E_{s,a}$ values. Similar results were obtained for NaBr and NaI solutions (data are not included here).

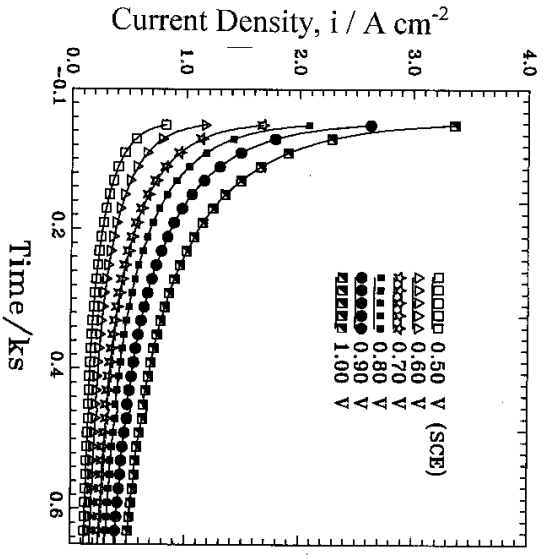

Figure 10. Potentiostatic current/time transients recorded for Ag electrode in 0.30 M NaCl solution at 25°C and at various anodic step potentials ($E_{s,a}$).

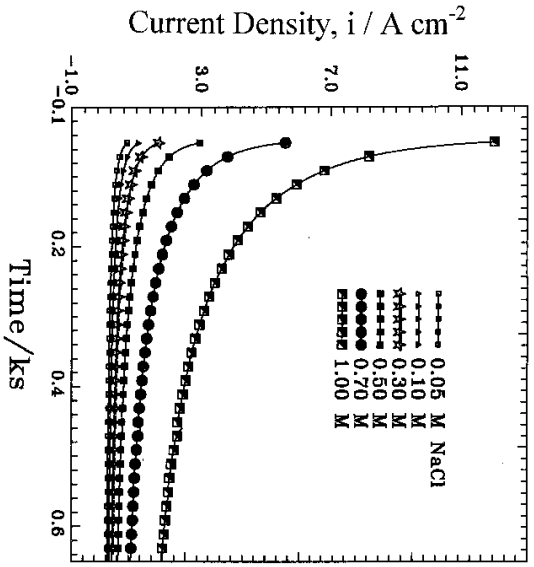

Figure 11. The influence of NaCl concentration on the potentiostatic current/time transients recorded for Ag electrode at $E_{s,a}$ = 0.70 V and at 25°C.

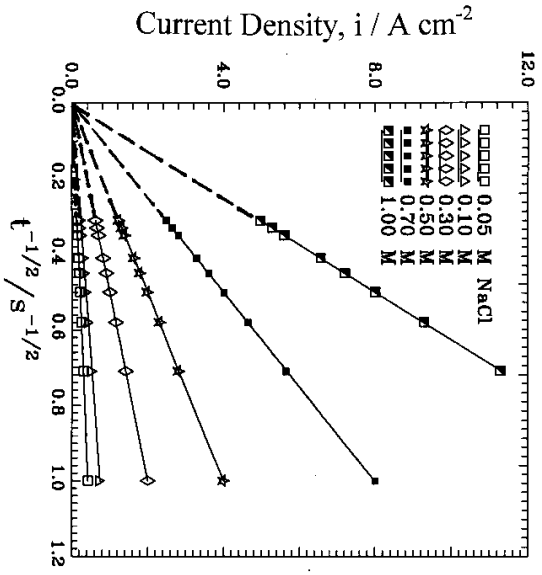

Figure 12. Dependence of the current density on $t^{-1/2}$ for the descending portions of the current transients recorded for Ag electrode in various concentrations of NaCl solution at $E_{s,a}$ = 0.70 V and at 25°C.

The influence of NaCl concentration and temperature on the i/t characteristics of Ag electrode at $E_{s,a}$ = 0.70 V has been studied, and some examples are given in Fig. 11. Similar results were obtained for NaBr and NaI solutions. Inspections of the obtained data reveal that the transient current density decreases monotonically with time reaching quasi steady-state current values. The values of the instantaneous and steady-state current densities increase by increasing either solution concentration or temperature, in addition to $E_{s,a}$. indicating an increase in the thickness of the anodically formed AgX layers. These results confirm the results obtained from cyclic voltammetric measurements.

In all cases it is found that, the continuously falling current was linear versus $t^{-1/2}$ passing through the origin; as shown in Fig. 12 as a representative example. These linear relations suggest that the growth of AgX layers is a diffusion controlled process and obeys the following equation [24,25].

$$i = P/t^{1/2} \qquad (15)$$

where $P = (z\ C\ D^{1/2}\ M^{1/2} / \pi^{1/2})$, z is the number of exchanged electrons, D, C and M are the diffusion coefficient, the concentration and the molecular weight of the diffusing species, respectively. The value of the slope (P) is a measure of the rate of AgX growth [26]. The numerical values of the slopes of the lines were calculated for Ag electrode under the influence of various operating variables, and the data are summarized in Tables 3-5. It follows from these data that, the slopes of the lines depend on the operating variables and the type of the halide ion. The values of the slopes (and hence the rate of AgX growth) increase by increasing either anodic step potential, halide concentration, or temperature. The values of P for the three halide ions under the same experimental conditions decrease in the order: $I^- > Br^- > Cl^-$. These results indicate that, the rate of AgX growth decreases in the same sequence.

Table 3. Values of the slopes of the lines for Ag electrode at $E_{s,a}$ = 0.70 V and at 25^{o}C under the influence of increasing NaX concentration.

	Slope (P)		
[X$^-$] / M	**Cl$^-$**	**Br$^-$**	**I$^-$**
0.05	0.43	0.59	0.87
0.10	0.75	1.02	1.25
0.30	2.02	2.75	3.24
0.50	4.00	5.88	6.77
0.70	7.88	9.05	9.95
1.00	15.45	17.44	19.11

Table 4. Values of the slopes of the lines for Ag electrode at in 0.30 M NaX solution at $E_{s,a}$ = 0.70 V under the influence of increasing solution temperature.

	Slope (P)		
Temp / ^{o}C	**Cl$^-$**	**Br$^-$**	**I$^-$**
15	1.13	1.87	2.17
25	2.02	2.75	3.24
35	3.08	4.14	5.50
45	5.22	6.13	6.98
55	6.84	7.55	8.54
65	7.19	8.66	9.84

4. CONCLUSIONS

(i) Comparative studies of the electrochemical behaviour of Ag in aqueous NaCl, NaBr and NaI solutions have been investigated by means of cyclic voltammetric and potentiostatic current/time transient techniques complemented with SEM observations.

(ii) The first cyclic voltammograms of Ag electrode in the three halide solutions are nearly similar and characterized by the occurrence of a broad anodic peak (AI) corresponding to the formation of AgX film (X^- = Cl^-, Br^-, I^-) on the anode surface.

(iii) The electroformation of AgX film is found to be limited by diffusion of X^- from the bulk solution to the electrode interface.

(iv) The peak current density of peak AI enhances by increasing X^- concentration, potential scan rate and solution temperature.

(v) Under similar experimental conditions, the peak current density of peak AI decreases in the order: $I^- > Br^- > Cl^-$.

(vi) For NaCl and NaBr solutions, the reverse potential scan exhibits a sharp cathodic peak CI in the cathodic part of the voltammogram, while for NaI solution, the reverse potential scan

exhibits an activation anodic peak in addition to the cathodic peak. The cathodic peaks CI are related to the electroreduction of AgX formed during the anodic process.

(vii) The apparent activation energies for the formation and reduction of AgX film decrease in the order: $Cl^- > Br^- > I^-$.

(viii) Current/time transient measurements show that the rate of AgX growth decreases in the order: $I^- > Br^- > Cl^-$.

(ix) SEM examinations of AgX films indicate that, the AgI film is highly porous and associated with large microcrakes as compared to AgBr and AgCl films.

References

1. M.A.M. Ibrahim, H.H. Hassan, S.S. Abdel-Rehim and M.A. Amin, *J Solid State Electrochem*., 3 (1999) 380.
2. S.S. Abdel-Rehim, H.H. Hassan, M.A.M Ibrahim and M.A. Amin, *Monatshefte fur Chemie*, 130 (1999) 1207.
3. S.S. Abdel-Rehim, M.A.M. Ibrahim, H.H. Hassan, M.A. Amin, *Can. J Chem*., 76 (1998) 1156
4. S.S. Abdel-Rehim, H.H. Hassan, M.A.M Ibrahim and M.A. Amin, *Monatshefte fur Chemie*, 129 (1998) 1103.
5. D. Ives, G. Janz, Reference Electrodes, Academic Press, London 1961.
6. R.F. Amlie, H.N. Honer, P. Reutschi, *J Electrochem.Soc*., 112 (1965) 1073.
7. D.W. Faletti, W.H. Gackstettera *J Electrochem.Soc*., 115 (1968) 1210.
8. D.R. Zielke, J.M. Brady, C.E. del Rio, *J Endodontics*, 11 (1975) 357.
9. S.S. Djokic, R.E. Burrell, *J Electrochem.Soc*., 145 (1998) 1426.
10. M.F.L. de Mele, R.C. Salvarezza, V.D.M. Vasquez, H.A. Videla, A.J. Arvia, *J Electrochem. Soc*., 133 (1986) 173.
11. V.I. Birss, G.A. Wright, *Electrochim. Acta*, 27 (1982) 1429.
12. V.I. Birss, G.A. Wright, *Electrochim. Acta*, 27 (1982) 1439.
13. L.J. Kurtz, Compt.Rend.*U.R.S.S*., 11 (1935) 383.
14. G.W. Briggs, H.R. Thirsk, *Trans Faraday Soc*., 48 (1952)1171.
15. W. Jaenicke, R. Tischer, H. Gerischer, *Z Elektrochem* , 59 (1955) 448.
16. W. Jaenicke, *Z. Elektrochem*., 55 (1951) 186.
17. S.A. Awad, *J Electroanal. Chem*., 21 (1969) 483.
18. M. Fleischmann, H. Thirsh, *Electrochim. Acta*, 1 (1959) 146.
19. D.A. Vermilyca, *Advan. Electrochem. Eng*., 3 (1963) 211.
20. R.C. Weast (ed.), Handbook of Chemistry and Physics (55 th edn)., Chemical Rubber Company, Boca Raton, 1974-1976 U.S.A.
21. P. Delahay, New Instrumental Methods in Electrochemistry, Interscience Publ., New York, 1954, P. 124.
22. M.K. Gomma, M.H. Wahdan Materials *Chemistry and Physics*, 39 (1995) 209.
23. J. Marsh, Advanced Organic Chemistry, 3rd ed., Wiley Eastern, New Delhy, 1988.
24. J.B. Randles, *Trans Farady Soc*., 44 (1948) 327.
25. A. Sevcik, *Collect Czech Chem Commun*., 13 (1948) 349.
26. G.E. Thomson, G.C. Wood, R. Hutchings, *Trans. Inst. Metal. Finish*., 58 (1980) 80.